Properties of Tetrahydropteroylpentaglutamate Bound to 10-Formyltetrahydrofolate Dehydrogenase†

Dong Woon Kim, Teng Huang, Douglas Schirch, and Verne Schirch*

Department of Biochemistry and Molecular Biophysics, Virginia Commonwealth University, Richmond, Virginia 23298-0614

Received August 6, 1996; Revised Manuscript Received September 26, 1996⊗

ABSTRACT: A new rapid procedure for purifying 10-formyltetrahydrofolate dehydrogenase results in 90 mg of pure enzyme from two rabbit livers. This abundant liver enzyme is known to bind its product tetrahydropteroylpentaglutamate ($H_4PteGlu_5$) so tightly that it does not dissociate during size exclusion chromatography. 10-Formyltetrahydrofolate dehydrogenase is also known to exhibit strong product inhibition by $H_4PteGlu_5$. There is a several-fold excess of 10-formyltetrahydrofolate dehydrogenase subunits in liver relative to the concentration of $H_4PteGlu_n$, suggesting that *in vivo* this enzyme may bind significant amounts of this coenzyme in a nearly irreversible enzyme·$H_4PteGlu_5$ complex. How this tightly bound $H_4PteGlu_n$ is transferred to the other two enzymes in the cytosol, serine hydroxymethyltransferase and C_1-tetrahydrofolate synthase, which use $H_4PteGlu_5$ as a substrate, is the subject of this investigation. Analysis of the product inhibition curve for 10-formyltetrahydrofolate dehydrogenase shows that H_4-$PteGlu_5$ has a dissociation constant near 15 nM which is 60-fold lower than the K_s for 10-formyl-H_4-$PteGlu_5$. Fluorescence titration studies also yield a K_d of about 20 nM for $H_4PteGlu_5$. Coupling the 10-formyltetrahydrofolate dehydrogenase reaction to an excess of either serine hydroxymethyltransferase or C_1-tetrahydrofolate synthase not only abolishes product inhibition but also increases the initial rate of its activity by about 2-fold. Passage of a reaction mixture of 10-formyltetrahydrofolate dehydrogenase down a size exclusion column results in enzyme with 1 equiv of $H_4PteGlu_5$ bound per subunit. However, addition of either serine hydroxymethyltransferase or C_1-tetrahydrofolate synthase results in a rapid transfer of this bound folate to these enzymes. Evidence is also presented that the tightly bound folate is in equilibrium with solvent $H_4PteGlu_5$.

Mammalian liver cells contain high concentrations of homotetrameric cytosolic 10-formyltetrahydrofolate dehydrogenase[1] (10-CHO-THF dehydrogenase, EC 1.5.1.6) which catalyzes the irreversible oxidation of 10-CHO-$H_4PteGlu_n$ to CO_2 and $H_4PteGlu_n$ (eq 1) (Kutzbach & Stokstad, 1971; Rios-Orlandi et al., 1986; Scrutton & Beis, 1979; Cook & Wagner, 1982; Min et al., 1988; Cook et al., 1991). This enzyme also catalyzes two additional reactions (eqs 2 and 3) (Krupenko et al., 1995; Schirch et al., 1994). It is not clear if the hydrolase activity (eq 2) and propanal dehydrogenase activity (eq 3) are of physiological importance. Recent studies have shown that each monomer of 10-CHO-THF dehydrogenase is composed of two independently folded domains. Proteolytic digestion gives a 32 kDa fragment which binds 10-CHO-$H_4PteGlu_n$ and catalyzes only reaction 2. A larger 63 kDa domain binds $NADP^+$ and propanal and catalyzes only reaction 3 (Cook et al., 1991; Schirch et al., 1994). However, to catalyze reaction 1, the two domains must be connected by a linker peptide (Schirch et al., 1994).

$$\text{10-CHO-}H_4\text{PteGlu}_n + NADP^+ \rightarrow H_4\text{PteGlu}_n + CO_2 + NADPH \quad (1)$$

$$\text{10-CHO-}H_4\text{PteGlu}_n \rightarrow H_4\text{PteGlu}_n + \text{formate} \quad (2)$$

$$\text{propanal} + NADP^+ \rightarrow NADPH + \text{propanoate} \quad (3)$$

Rat and pig liver 10-CHO-THF dehydrogenases have been shown to bind $H_4PteGlu_5$ and $H_4PteGlu_6$ very tightly with the coenzyme remaining bound during size exclusion chromatography (Cook & Wagner, 1982; Min et al., 1988). Recently, *in vivo* evidence has been presented that the rat enzyme also binds the substrate 10-CHO-$H_4PteGlu_n$ tightly and that the hydrolase activity slowly converts the tightly bound substrate to tightly bound $H_4PteGlu_n$ (Wagner et al., 1995). *In vitro* kinetic studies suggest that 10-CHO-THF dehydrogenases exhibits strong product inhibition. It has been assumed that product inhibition is related to the H_4-$PteGlu_n$ tight binding properties of 10-CHO-THF dehydrogenases.

Previous studies have proposed that 10-CHO-THF dehydrogenase represents about 0.5−1.0% of the soluble protein in mammalian liver (Cook et al., 1991). This suggests that the intracellular concentration of 10-CHO-THF dehydrogenases exceeds the concentration of $H_4PteGlu_n$ and that *in vivo* most, if not all, of the folate pool in the form of H_4-

† This work was supported by Grant GM 28143 from the National Institutes of Health.

* To whom correspondence should be addressed. Telephone: 804-828-9482. Fax: 804-828-3093. E-mail: schirch@gems.vcu.edu.

⊗ Abstract published in *Advance ACS Abstracts,* November 15, 1996.

[1] Abbreviations: 10-CHO-THF dehydrogenase, 10-formyltetrahydrofolate dehydrogenase; SHMT, serine hydroxymethyltransferase; C_1-THF synthase, C_1-tetrahydrofolate synthase; $H_4PteGlu_n$, tetrahydropteroylglutamate containing *n* glutamate residues; 10-CHO-$H_4PteGlu_n$, 10-formyltetrahydropteroylglutamate; 5,10-CH^+-$H_4PteGlu_n$, 5,10-methenyltetrahydropteroylglutamate; 5-CHO-$H_4PteGlu_n$, 5-formyltetrahydropteroylglutamate; 5,10-CH_2-$H_4PteGlu_n$, 5,10-methylenetetahydropteroylglutamate; 10-CHO-5,8-dideazafolate, 10-formyl 5,8-dideazafolate; EDTA, ethylenediaminetetraacetic acid; KP_i, potassium phosphate; DTT, dithiothreitol.

S0006-2960(96)01968-X CCC: $12.00

Scheme 1: Metabolic Cycles Involving 10-CHO-THF Dehydrogenase, SHMT, and C_1-THF Synthase[a]

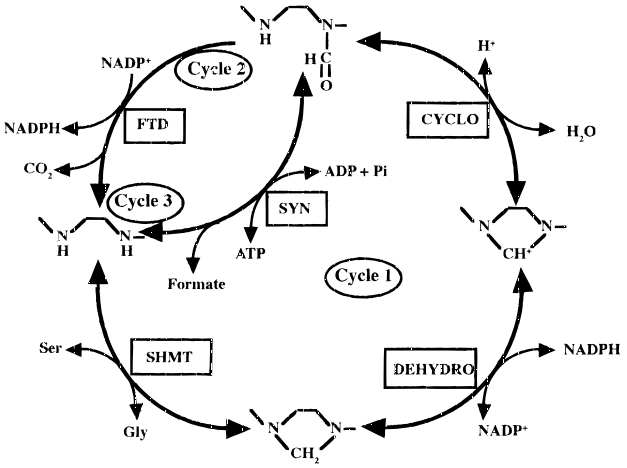

[a] Cycle 1 involves the conversion of formate and $H_4PteGlu_5$ (or any folate intermediate involved in the cycle) to serine with the regeneration of $H_4PteGlu_5$. The two enzymes involved are SHMT and the three activities of C_1-THF synthase (DEHYDRO, 5,10-CH_2-THF dehydrogenase; CYCLO, 5,10-CH^+-THF cyclohydrolase; and SYN, 10-CHO-THF synthetase). The rate of cycle 1 is determined by the decrease in absorbance at 340 nm due to the oxidation of NADPH. Cycle 2 involves only 10-CHO-THF dehydrogenase and the 10-CHO-THF synthetase activity of C_1-THF synthase. This cycle oxidizes formate to CO_2 with the reduction of $NADP^+$ to NADPH which is used to follow the rate. Either 10-CHO-$H_4PteGlu_5$ or $H_4PteGlu_5$ can be used as the substrate at catalytic levels.

$PteGlu_n$ may be bound to the enzyme (Cichowicz & Shane, 1987; Horne et al., 1989; Strong & Schirch, 1989). This raises the question of how other reactions which require $H_4PteGlu_n$ as a substrate can compete with 10-CHO-THF dehydrogenases for this compound. There are two major enzymes in liver cytosol which require $H_4PteGlu_n$ as a substrate. SHMT converts serine and $H_4PteGlu_n$ to glycine and 5,10-CH_2-$H_4PteGlu_n$, and 10-CHO-THF synthetase catalyzes the formation of 10-CHO-$H_4PteGlu_n$ from $H_4PteGlu_n$ and formate (Schirch, 1982; Strong & Schirch, 1989). This later enzyme is one activity of the trifunctional enzyme C_1-THF synthase.

SHMT, C_1-THF synthase, and 10-CHO-THF dehydrogenase form two metabolic cycles that interconvert $H_4PteGlu_n$ and 10-CHO-$H_4PteGlu_n$ (referred to as cycles 1 and 2 in Scheme 1). Cycle 1 involves SHMT and the three activities of C_1-THF synthase and is reversible. 10-CHO-THF dehydrogenase and the 10-CHO-THF synthetase activity form cycle 2 which operates in only one direction because of the irreversibility of the dehydrogenase-catalyzed reaction. If previous studies on the abundance of 10-CHO-THF dehydrogenase in liver are correct, then the concentration of this enzyme exceeds by a factor of at least 1.5 the combined concentrations of SHMT and C_1-THF synthase (Strong & Schirch, 1989).

Using purified enzymes, this study determines both the affinity and stoichiometry of the 10-CHO-THF dehydrogenase·$H_4PteGlu_5$ complex. The relationship of tight binding of $H_4PteGlu_5$ and the kinetic properties of 10-CHO-THF dehydrogenase are also examined. Also described is how 10-CHO-THF dehydrogenase, SHMT, and C_1-THF synthase compete for $H_4PteGlu_5$. The results suggest that the kinetic properties of the three enzymes when combined cannot be explained by the sum of their individual kinetic properties.

EXPERIMENTAL PROCEDURES

Materials. All coenzymes, buffers, heparin−agarose, coupling reagents, and amino acids were obtained from Sigma. [2-^{3}H]Glycine (10 Ci/mmol) was from Amersham Corp. 5,8-Dideazafolic acid and 10-CHO-5,8-dideazafolic acid were purchased from Dr. John Hynes, University of South Carolina. 5-CHO-$H_4PteGlu_5$ was prepared as previously described from $PteGlu_5$ purchased from Schircks Laboratories (Jona, Switzerland) (Stover & Schirch, 1992). 5-^{14}CHO-$H_4PteGlu_5$ was prepared from [^{14}C]formate and 5-CHO-$H_4PteGlu_5$ by a previously published formyl exchange reaction (Stover & Schirch, 1992). 10-CHO-$H_4PteGlu_5$ was prepared from 5-CHO-$H_4PteGlu_5$ by first converting it to 5,10-CH^+-$H_4PteGlu_5$ in acid and then incubating at neutral pH (Stover & Schirch, 1992). Rabbit liver cytosolic SHMT and C_1-THF synthase were purified from fresh frozen rabbit livers obtained from Pel-Freeze Biologicals (Rogers, AK) and stored in 10% glycerol at −70 °C (Stover and Schirch, 1992). Mouse folylpolyglutamate synthetase was a generous gift from Dr. Richard Moran (Virginia Commonwealth University).

The polyglutamate forms of 5,8-dideazafolate were prepared by incubation with folylpolyglutamate synthetase and ATP according to the method of Moran & Colman (1984). The individual polyglutamate forms were purified by HPLC on a C-18 reverse phase column (Moran & Colman, 1984). [3,4-^{3}H]Glutamate (41 Ci/mmol from Moravek) was used to make the tritium-labeled polyglutamate derivatives of 5,8-dideazafolate. The 5,8-dideazafolate affinity column was prepared by the method of Grimshaw et al. (1984).

Purification of 10-CHO-THF Dehydrogenase. Two frozen rabbit livers were broken into small pieces with a hammer, briefly thawed, and homogenized in a Waring blender for 2 min in 400 mL of 50 mM KP_i, 0.3 M sucrose, 14 mM 2-mercaptoethanol, 1 mM EDTA, and 0.5 mM DTT at pH 7.25. The homogenate was centrifuged for 30 min at 9000 rpm and the pellet discarded. After removal of the floating lipids by passage through glass wool, ammonium sulfate was added to 30% of saturation (176 g/L). This solution was stirred on ice for 20 min, and the precipitated proteins were removed by centrifugation at 9000 rpm for 30 min. Ammonium sulfate was added to the supernatant to 55% of saturation (162 g/L), and after being stirred for 20 min, the solution was centrifuged for 30 min. The pellet was resuspended in 300 mL of 10 mM KP_i, 14 mM 2-mercaptoethanol, 1 mM EDTA, and 0.5 mM DTT at pH 6.8 (buffer A). The high salt content was lowered by repeated passage through a Pelicon apparatus until the conductivity reached 5000 μS. The desalted solution was then applied to a 5 × 7 cm CM-Sephadex column equilibrated with buffer A. Hemoglobin sticks to CM-Sephadex under the conditions used, but 10-CHO-THF dehydrogenase activity passes through. The eluate was then loaded on a 7 × 7 cm heparin−agarose column equilibrated with buffer A. The column was washed extensively with 1 L of buffer A followed by a linear gradient of 500 mL of buffer A and 500 mL of 0.5 M KCl in 50 mM KP_i, 14 mM mercaptoethanol, 1 mM DTT, and 1 mM EDTA at pH 7.3. Fractions (25 mL) were collected, and the 10-CHO-THF dehydrogenase activity was found near the beginning of the gradient. Ammonium sulfate was added to the pooled fractions, about 200 mL, to 60% of saturation, and the suspension was kept

at 4 °C overnight. The next morning, the solution was centrifuged at 9000 rpm for 25 min and the pellet dissolved in a minimal amount of 50 mM KP_i at pH 7.25 containing 1 mM EDTA, 0.5 mM DTT, and 14 mM 2-mercaptoethanol. The solution was desalted by passing it through a 4 × 20 cm Sephadex G-25 column equilibrated with the 50 mM potassium phosphate buffer. The desalted sample was then loaded onto a 3 × 9 cm 5,8-dideazafolate Sepharose-4B affinity column equilibrated with the same buffer. After the column was washed with 300 mL of equilibration buffer or until the A_{280} was less than 0.1, it was washed with 300 mL of 1 M KCl in equilibration buffer. 10-CHO-THF dehydrogenase was then eluted with 200 mL of 100 μM 5,8-dideazafolate and 1 M KCl in the equilibration buffer. Fractions (5 mL) were collected and those containing 10-formyltetrahydrofolate dehydrogenase activity pooled. Ammonium sulfate was added to 60% of saturation and the solution centrifuged at 9000 rpm for 25 min. The pellet was dissolved in a small amount of 20 mM KP_i (pH 7.2), 3 mM DTT, 14 mM 2-mercaptoethanol, and 20% glycerol and dialyzed against this buffer overnight. The enzyme was stored at −20 °C.

The concentration of 10-CHO-THF dehydrogenase was determined from its absorbance at 278 nm using the relationship of $0.9A_{278}$ equals 1 mg/mL 10-CHO-THF dehydrogenase. This value was previously determined from both weight measurements of protein samples and amino acid analysis (Schirch et al., 1994).

Determination of $H_4PteGlu_5$ Concentrations. The amount of $H_4PteGlu_5$, either bound to 10-CHO-THF dehydrogenase or as a contaminant in solutions of 10-CHO-$H_4PteGlu_5$, was determined by taking advantage of a previously used assay involving the $H_4PteGlu$-dependent solvent exchange of the 2-*pro-S* proton of glycine by SHMT (Chen & Schirch, 1973). $H_4PteGlu_n$ bound to 10-CHO-THF dehydrogenase was determined by taking 5 nmol of enzyme and boiling in 20 mM potassium phosphate at pH 7.3 containing 20 mM sodium ascorbate and 10 mM 2-mercaptoethanol. The precipitated protein was removed by centrifugation and the supernatant added to a solution of [^{3}H]glycine (1.5×10^6 cpm) and SHMT (0.5 mg) and incubated at 30 °C. After 3 min, 10 μL of a 10% solution of trichloroacetic acid was added to stop the reaction and to lower the pH of the solution. This solution was then added to a 1 cm high column of Dowex-50 in a 1 mL plastic syringe that had been equilibrated with 10 mM HCl. After the reaction solution had been absorbed, a vial containing 7 mL of Scintiverse (Fisher Scientific) scintillation fluid was placed under the column and the column washed with three successive aliquots of 200 μL of 10 mM HCl. The vials were then counted for ^{3}H. In the presence of 10 mM HCl, the cationic glycine remains bound to the column but the ^{3}H exchanged with solvent passes through the column into the counting vial. A standard curve is constructed by adding known concentrations of $H_4PteGlu_n$ to the assay solution. The assay is linear with $H_4PteGlu_n$ between 1 and 100 pmol. No other N^5- or N^{10}-substituted $H_4PteGlu_n$ derivative enhances the SHMT catalysis of the solvent exchange of the 2-*pro-S* proton of glycine. However, 10-CHO-$H_4PteGlu_n$ can also be determined by first incubating the solution with $NADP^+$ and 10-CHO-THF dehydrogenase to convert this substrate to $H_4PteGlu_n$.

Enzyme Assays. All assays for the determination of 10-CHO-THF dehydrogenase activity for reactions 1−3 (eqs 1−3) were performed at 30 °C as previously described (Schirch et al., 1994). The rate of the hydrolase reaction is proportional to the concentration of 2-mercaptoethanol. In the assay solution, this thiol was used at 100 mM. For assay reaction 3, 30 mM propanal was substituted for 10-CHO-$H_4PteGlu_5$ and the buffer was 60 mM sodium pyrophosphate at pH 8.5. For some studies, 0.2 mM 10-CHO-5,8-dideazafolate replaced 10-CHO-$H_4PteGlu_5$ as the substrate. This analog has been shown to be an effective substrate for 10-CHO-THF dehydrogenase (Krupenko et al., 1995).

The effect of SHMT and C_1-tetrahydrofolate synthase on the initial velocity of the dehydrogenase activity of 10-CHO-THF dehydrogenase was determined in a stopped-flow spectrophotometer from Kinetic Instruments, Inc. One syringe contained 10-CHO-THF dehydrogenase (2 μM) in 50 mM Tris (pH 7.5) containing 20 mM 2-mercaptoethanol. The second syringe contained in this buffer 10 μM (6R)-10-CHO-$H_4PteGlu_5$ and 300 μM $NADP^+$. To determine the effect of SHMT on the initial velocity, the second syringe also included 4 μM rabbit cytosolic SHMT subunits and 30 mM L-serine. To determine the effect of C_1-THF synthase on the initial rate of the 10-CHO-THF dehydrogenase reaction, the second syringe included 4 μM C_1-THF synthetase, 20 mM ammonium formate, and 5 mM MgATP.

New activity assays in this study include the combination of the enzymes 10-CHO-THF dehydrogenase, SHMT, and C_1-THF synthase. This last enzyme catalyzes three separate reactions as shown in Scheme 1. These reactions are the methylenetetrahydrofolate dehydrogenase activity (DEHYDRO), the methenyltetrahydrofolate cyclohydrolase activity (CYCLO), and the 10-formyltetrahydrofolate synthetase activity (SYN). The set of reactions involving SHMT and C_1-tetrahydrofolate synthase is referred to in the text and Scheme 1 as cycle 1 with the folate substrates functioning at catalytic levels. Each reaction is reversible in cycle 1. The reaction was performed in 1 mL of 20 mM potassium phosphate buffer at pH 7.3 with 14 mM 2-mercaptoethanol, 2 mM MgATP, 0.2 mM NADPH, 4 mM ammonium formate, 20 mM glycine, 0.135 mg of C_1-THF synthase (1.2 nmol), 0.145 mg of SHMT (2.7 nmol), and 50−250 pmol of either 10-CHO-$H_4PteGlu_5$ or $H_4PteGlu_5$. The reaction was initiated with C_1-THF synthase, and the decrease in absorbance of a 336−346 nm window was followed for about 1 min at 30 °C. The spectrophotometer software continuously subtracted a 436−446 nm absorbance window to correct for random light scattering. Absorbance changes as low as 0.01 min^{-1} could be accurately followed. Each assay was performed several times with the standard deviation usually smaller than the size of the symbol used in Figure 6. Under these assay conditions, the rate of NADPH disappearance is equivalent to the folate being cycled about 50 times per minute.

An additional combination of reactions is 10-CHO-THF dehydrogenase (eq 1) and the 10-formyltetrahydrofolate synthetase activity of C_1-THF synthase (cycle 2 in Scheme 1). This reaction was also performed in 1 mL of 50 mM Tris buffer at pH 7.5 with 0.2 mM $NADP^+$, 2 mM MgATP, 4 mM ammonium formate, 150 μg of 10-CHO-THF dehydrogenase (1.5 nmol), 175 μg of C_1-THF synthase (1.6 nmol), and 90−250 pmol of 10-CHO-$H_4PteGlu_5$. The reaction was started with the addition of C_1-THF synthase and the increase in absorbance at 340 nm determined over the first minute of the reaction as described above for the reactions in cycle 1.

Product Inhibition Studies. Both the dehydrogenase and hydrolase activities of 10-CHO-THF dehydrogenase were analyzed for product inhibition. The reactions were performed on a stopped-flow spectrophotometer from Kinetic Instruments, Inc., at 30 °C. The buffer was 50 mM Tris/HCl at pH 7.5 with 10 mM 2-mercaptoethanol for the dehydrogenase reaction and 100 mM 2-mercaptoethanol for the hydrolase reaction. 10-CHO-THF dehydrogenase (0.25 μM) was flowed against 10-CHO-H_4PteGlu$_n$ with n equal to 1 or 5. For the monoglutamate, the concentration of 10-CHO-H_4PteGlu was 100 μM, and for the pentaglutamate derivative, the concentration was 5−7 μM. For the dehydrogenase reaction, the enzyme syringe also contained a $NADP^+$-regenerating system of 400 μM $NADP^+$, 60 mM ammonium sulfate, 10 mM α-ketoglutarate, and 17 units of glutamate dehydrogenase. The dehydrogenase and hydrolase reactions (eqs 1 and 2) were monitored at 340 and 295 nm, respectively (Schirch et al., 1994).

The absorbance versus time curve was used to calculate the rate of the reaction at 20 s intervals and to determine the concentration of substrate and product at each interval. The initial rate during the first 10 s was used to estimate the value of V_{max}. The results were plotted as v versus 10-CHO-H_4PteGlu$_n$ concentration for the equation of the product as a competitive inhibitor of substrate binding as shown in eq 4 (Segel, 1975). The data points were then fit to eq 4 for product inhibition using PSI-Plot software with V_{max} fixed and the curve fit to determine the best values for K_s and K_p.

$$v/V_{max} = [S]/K_s(1 + [P]/K_p) + [S] \quad (4)$$

Fluorescence Titration. The K_d and stoichiometry of H_4PteGlu$_5$ binding to 10-CHO-THF dehydrogenase were determined by observing the quenching of Trp fluorescence during titration of the enzyme with H_4PteGlu$_5$ as previously described for the monoglutamate form of the coenzyme (Schirch et al., 1994). Data were collected on a Shimadzu RF 5000U spectrofluorimeter with 5 nm slit widths. Experiments were performed at 23 °C in argon-purged 50 mM Tris/HCl, 2 mM DTT, and 10 mM 2-mercaptoethanol at pH 7.5. 10-CHO-THF dehydrogenase (0.25−0.49 μM) was titrated with 1−5 μL aliquots of (6*S*)-H_4PteGlu$_5$ (33−330 μM) until the protein was nearly saturated with ligand. The samples were excited at 290 nm, and emission was monitored at 340 nm. Both dilution effects, due to the addition of the ligand, and inner filter effects were less than 2%.

Stoichiometry of Folate Binding to 10-CHO-THF Dehydrogenase. A variety of methods were used to determine the amount of different folate compounds and folate analogs which were bound tightly to 10-CHO-THF dehydrogenase. In each method, the folate compounds or analogs were incubated with the enzyme in 20 mM Tris/HCl at pH 7.5 containing 14 mM 2-mercaptoethanol and 1 mM DTT. This will be referred to as the Tris buffer. In one method, this 10-CHO-THF dehydrogenase folate mixture was chromatographed on a 1 × 20 cm column of Sephadex G-25 or DG-P6 Sepharose equilibrated with Tris buffer at pH 7.5. Fractions (0.6 mL) were collected and analyzed for both absorbance and bound folate. To determine the amount of bound folate, a difference spectrum between a 10 μM solution of 10-CHO-THF dehydrogenase (without bound H_4PteGlu$_5$) and after the addition of 2 μM H_4PteGlu$_5$ was taken. It is assumed that all of the H_4PteGlu$_5$ is bound under these conditions. The difference spectrum showed a broad peak with a maximum at 300 nm. From this difference absorbance spectrum of the bound H_4PteGlu$_5$, the values for ϵ_{316nm} and ϵ_{280nm} were both 27 mM^{-1} cm^{-1}. The A_{316} was used to calculate the H_4PteGlu$_5$ concentration because the protein does not absorb at this wavelength. The A_{316} absorbance value was subtracted from the absorbance at 280 nm of the complex, which is the sum of the absorbance of enzyme and bound folate, before calculating the 10-CHO-THF dehydrogenase concentration (Figure 5B shows the spectrum of enzyme with and without bound H_5PteGlu$_5$).

When tritium-labeled 5,8-dideazafolate was used as the ligand, the specific activity was calculated from the spectrum of the compound and its counts per minute determined in a liquid scintillation counter. The stoichiometry for the 10-CHO-THF dehydrogenase·5,8-dideazafolate complex was then determined by counting the fractions from the size exclusion column to determine the folate concentration and using the A_{280} to determine the 10-CHO-THF dehydrogenase concentration.

Transfer of 10-CHO-THF Dehydrogenase-Bound H_4PteGlu$_5$ to SHMT. The 10-CHO-THF dehydrogenase·H_4PteGlu$_5$ complex (10 μM) in 50 mM potassium phosphate at pH 7.3 containing 7 mM 2-mercaptoethanol, 5 mM DTT, and 30 mM glycine was placed in a syringe of a stopped-flow instrument and flowed against a solution of 80 μM rabbit cytosolic SHMT and 30 mM glycine in the same buffer at 23 °C. The formation of the SHMT·Gly·H_4PteGlu$_5$ ternary complex was monitored at 496 nm. In additional experiments, either 100 μM 5,8 dideazafolate or 100 μM 10-CHO-5,8-dideazafolate was added to the syringe containing SHMT and glycine.

RESULTS

Purification of 10-CHO-THF Dehydrogenase. Previous estimates have suggested that the 10-CHO-THF dehydrogenase concentration in liver is 0.5−1.0% of the total soluble protein (Cook & Wagner, 1982). Even though this makes it one of the most abundant proteins in liver cytosol, the purification of the enzyme by several different investigators took several days and gave poor yields (Cook & Wagner, 1982, 1986; Schirch et al., 1994). In this study, we report on the addition of two columns not used in previous methods. Even though the enzyme does not stick to CM-Sephadex at neutral pH, indicating it does not have a net positive charge, 10-CHO-THF dehydrogenase does bind to anionic heparin−agarose. The enzyme also binds very tightly to a 5,8-dideazafolic acid affinity column, being eluted only with 5,8-dideazafolate at high salt. These two columns have permitted the purification of 10-CHO-THF dehydrogenase from rabbit liver in 1.5 days with an overall yield of 24%. From two rabbit livers, we obtain 90 mg of enzyme that is greater than 95% pure as judged by SDS−PAGE (Table 1). This is a significant improvement over our previous procedure.

The purified enzyme shows a typical protein absorption maximum at 278 nm as shown by the solid line in Figure 5B. Using the H_4PteGlu$_n$-dependent exchange of the 2-*pro-S* proton of glycine by SHMT (Experimental Procedures), no detectable H_4PteGlu$_n$ or 10-CHO-H_4PteGlu$_n$ was found to be bound to a denatured 10 nmol sample of 10-CHO-THF dehydrogenase. This method detects as little as 1 pmol of

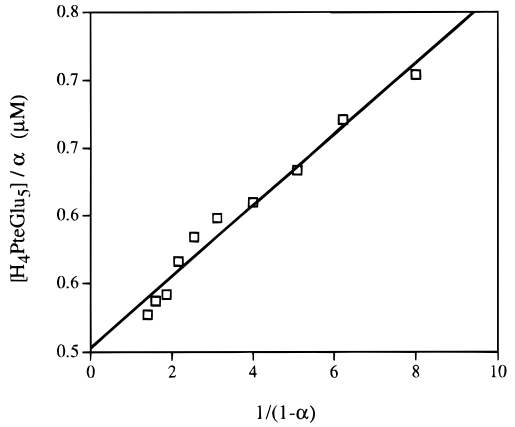

FIGURE 1: Titration of 0.49 μM 10-CHO-THF dehydrogenase with 50−400 μM $H_4PteGlu_5$ as monitored by fluorescence. The protein was excited at 290 nm and the emission monitored at 340 nm as described in Experimental Procedures. The data were analyzed according to the derivation of the Scatchard equation, $L_o/\alpha = K_d/(1 - \alpha) + E_o$, where L_o is the concentration of added ligand, α represents the fractional saturation of 10-CHO-THF dehydrogenase subunits as determined by Δfluorescence/maximal Δfluorescence, and E_o is the concentration of enzyme binding sites. Plotting L_o/α versus $1/(1 - \alpha)$ allows determination of the K_d (slope) and E_o (y-intercept). Dividing E_o by the concentration of 10-CHO-THF dehydrogenase subunits permits determination of n, the number of binding sites per subunit (Webb, 1963).

Table 1: Purification of 10-Formyltetrahydrofolate Dehydrogenase from Rabbit Liver

step	total protein (mg)	total activity (units)	specific activity (unit/mg)	recovery (%)
homogenate	29900	217	0.007	100
$(NH_4)_2SO_4$	16560	231	0.014	106
CM-Sephadex and heparin−agarose	504	100	0.20	46
5,8-dideazafolic acid affinity	91	53	0.58	24

either 10-CHO-$H_4PteGlu_n$ or $H_4PteGlu_n$ (Chen & Schirch, 1973).

K_d for $H_4PteGlu_5$. Tryptophan fluorescence of 10-CHO-THF dehydrogenase decreases by 50% with binding of $H_4PteGlu_5$. Analysis of the decrease in fluorescence in the presence of 0.49 μM enzyme and increasing $H_4PteGlu_5$ concentrations (Figure 1) yielded a K_d of 0.021 $\pm$ 0.004 μM and an n of 1.05 $\pm$ 0.06 per monomer (result of four separate experiments) when plotted using a derivation of the Scatchard equation as described previously (Webb, 1963). Experiments using 0.25 μM 10-CHO-THF dehydrogenase also gave the same result for n and K_d (data not shown). This result suggests that each subunit of the tetrameric enzyme binds one molecule of $H_4PteGlu_5$ and that the binding sites act independently. Previously, we had determined a K_d of 1.4 μM for $H_4PteGlu$ (Schirch et al., 1994). This shows that the addition of four glutamate residues to $H_4PteGlu$ decreases the K_d by about 70-fold.

Product Inhibition of 10-CHO-THF Dehydrogenase. Previous investigators have noted that both the dehydrogenase and hydrolase activities of 10-CHO-THF dehydrogenase decrease during the progress of an assay and that it cannot be explained as a depletion of the substrate concentration, suggesting that this enzyme shows product inhibition. Because of the putative strong product inhibition, it has not been possible to determine either the K_m for 10-CHO-$H_4PteGlu_5$ or the product dissociation constant, K_p, for $H_4PteGlu_5$.

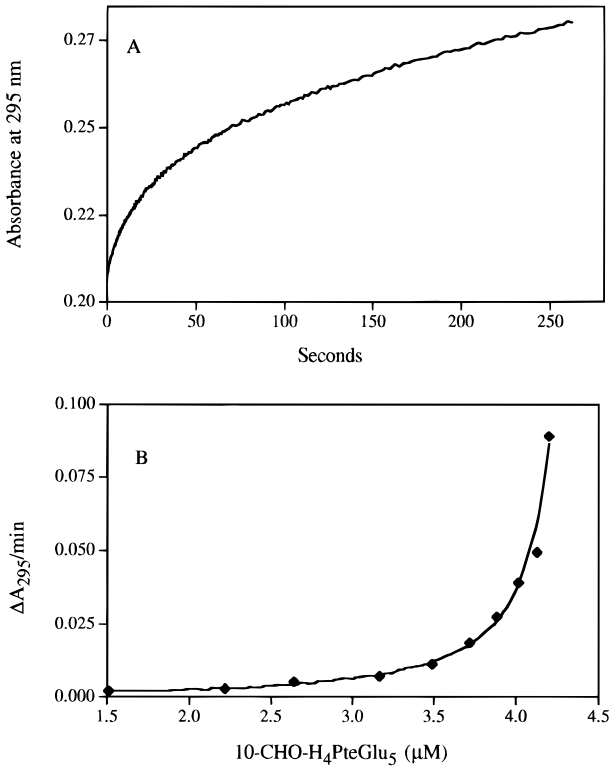

FIGURE 2: Product inhibition analysis of 10-CHO-THF dehydrogenase. (A) Progress of the hydrolase activity (eq 2) of 10-CHO-THF dehydrogenase during the conversion of 10-CHO-$H_4PteGlu_5$ to $H_4PteGlu_5$ by observing the increase in absorbance at 295 nm. The decreasing slope is primarily the result of product inhibition. (B) Analysis of the progress curve shown in part A using eq 4 for product inhibition (Segel, 1975). The diamonds are the slopes of the progress curve taken from part A, and the solid line is a curve fit of the data using an initial value for V_{max} of 0.2 absorbance unit/min. The curve fit gave a K_s value for 10-CHO-$H_4PteGlu_5$ of 0.9 μM and a K_p value for $H_4PteGlu_5$ of 15 nM.

As an approach to obtaining K_s for 10-CHO-$H_4PteGlu_n$ and K_p for $H_4PteGlu_n$, we studied the progress curve for the hydrolase activity that converts 10-CHO-$H_4PteGlu_5$ to $H_4PteGlu_5$ (eq 2). The reaction was started with a concentration of substrate which was about 8-fold higher than its estimated K_m value, and product formation was followed on a stopped-flow spectrophotometer to obtain a better estimate of the initial rate. This permitted estimating the V_{max} of the reaction from the initial rate and solving for K_s and K_p using eq 4. Figure 2A shows an absorbance versus time progress curve for the hydrolase reaction from a stopped-flow spectrophotometer trace starting with 4.1 μM 10-CHO-$H_4PteGlu_5$. The slope of the progress curve was determined every 20 s to obtain the rate of the reaction. From the molar absorbtivity coefficient for product formation, it was also possible to determine the concentration of both substrate and product for each 20 s interval. The rate versus substrate concentration data points were then plotted and curve fit for eq 4. The initial rate was almost double the value averaged over the first 20 s of the reaction. This is because product inhibition is significant by 20 s. Also, the K_s of the substrate was not as low as we had suspected, and the initial rate had to be increased slightly above the measured initial rate in order to find the best fit to the data. Figure 2B shows that the solid line, which is the curve fit from eq 4 with an estimated V_{max}

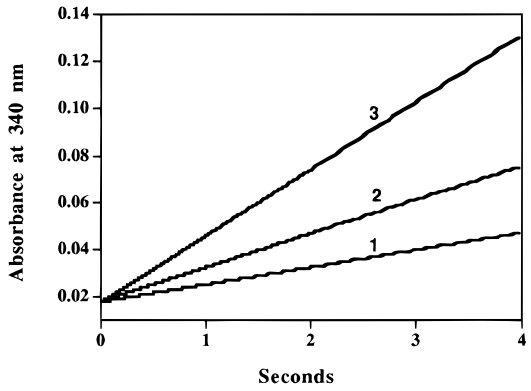

FIGURE 3: Initial velocity of 10-CHO-THF dehydrogenase in the presence of SHMT and C_1-THF synthase during the first 4 s of the reaction. (Curve 1) 10-CHO-THF dehydrogenase (2 μM) was flowed against excess $NADP^+$ and 14 μM 10-CHO-H_4PteGlu$_5$ and the rate of reaction determined by the increase in absorbance at 340 nm. (Curve 2) L-Serine (30 mM) and SHMT (4 μM) were included in the second syringe. (Curve 3) MgATP (2 mM), ammonium formate (4 mM), and C_1-THF synthase (4 μM)(were included in the second syringe.

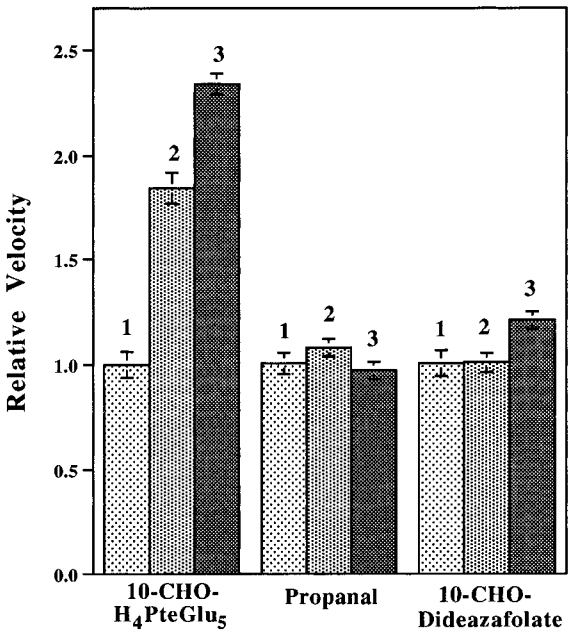

FIGURE 4: Relative initial velocities of 10-CHO-THF dehydrogenase in the presence of SHMT and C_1-THF synthase with different substrates. Column 1 is the relative initial velocity of 10-CHO-THF dehydrogenase for reaction 1 (eq 1). Column 2 employs the same assay conditions used to obtain the initial velocity recorded in column 1 with the addition of 20 mM L-serine and 200 μg of rabbit cytosolic SHMT. Column 3 is the same assay solution used to obtain the initial rate recorded in column 1 with the addition of 2 mM MgATP, 4 mM ammonium formate, and 200 μg of rabbit cytosolic C_1-THF synthase. The concentrations of the substrates for 10-CHO-THF dehydrogenase were as follows: 200 μM $NADP^+$, 70 μM (6*R*)-10-CHO-H_4PteGlu$_5$, 30 mM propanal, and 200 μM 10-CHO-dideazafolate.

of 0.2 AU/min, gives a reasonably good fit to the data points. From this curve, a value for K_s of 0.9 μM is obtained which is 60-fold higher than the determined K_p value of 0.015 μM.

The shape of the progress curve showed more product inhibition with the pentaglutamate form of the coenzyme than with the monoglutamate form, suggesting that the 15 nM value for K_p of H_4PteGlu$_5$ is much lower than the K_p of H_4-PteGlu, which could not be accurately determined by this method. A previous study using fluorescence titration, as described in Figure 1, gave a K_d value of 1.4 μM for H_4-PteGlu which is only 14-fold lower than the K_m of 20 μM for 10-CHO-H_4PteGlu (Schirch et al., 1994). However, the k_{cat} value of 52 min^{-1} is the same for both the monoglutamate and pentaglutamate forms of the substrate.

The hydrolase activity of 10-CHO-THF dehydrogenase was used for determining the product inhibition curve because fewer complications arise with it than with the dehydrogenase activity. It has been shown that the product NADPH activates the dehydrogenase activity, and this would add complications to interpretation of the data for product inhibition by H_4PteGlu$_5$. To estimate the kinetic constants from the progress curve using the dehydrogenase activity (eq 1), we added an $NADP^+$-regenerating system to the assay. Using this assay system, with the conditions described above for the hydrolase activity, we found essentially the same product inhibition pattern and the same values for K_s and K_p as determined for the hydrolase reaction.

Effect of SHMT and C_1-THF Synthase on the 10-CHO-THF Dehydrogenase Activity. SHMT and L-serine have previously been used to remove H_4PteGlu$_n$ as a product from the 10-CHO-THF dehydrogenase reaction (Schirch et al., 1994). Removal of H_4PteGlu$_n$ by this coupled enzyme system abolishes the product inhibition pattern, resulting in a linear increase in A_{340} versus time until substrate is nearly depleted. However, addition of SHMT and L-serine also increases the initial rate of the reaction by 1.8-fold with 10-CHO-H_4PteGlu$_5$ as substrate when analyzed in a stopped-flow spectrophotometer (Figure 3, curve 2). This increased rate was also observed for 10-CHO-H_4PteGlu$_5$ in a conventional assay which looks at the initial rate after 5 s (Figure 4, column 2). The same increased rate returned at any point in the 10-CHO-THF dehydrogenase reaction where SHMT and L-serine were added, confirming that the decrease in rate was not the result of substrate depletion for this irreversible reaction.

The results shown in Figures 3 and 4 are for the dehydrogenase activity of 10-CHO-THF dehydrogenase (eq 1), but the same effect on initial rate was observed with the hydrolase reaction (results not shown). Addition of serine or glycine with $NADP^+$ had no effect on the initial rate in these studies.

A possible explanation for this increase in initial velocity of the 10-CHO-THF dehydrogenase reaction, induced by SHMT and serine, is that the substrate 10-CHO-H_4PteGlu$_5$ is contaminated with a small amount of H_4PteGlu$_5$. Because the product binds 60-fold more tightly than the substrate, even a 1% contamination could cause some inhibition of the initial rate. The addition of SHMT and serine would remove this contaminating H_4PteGlu$_5$ and thus increases the initial rate. We tested for H_4PteGlu$_5$ in our 10-CHO-H_4PteGlu$_5$ solution by using the H_4PteGlu$_n$-dependent exchange of the 2-*pro-S* proton of glycine by SHMT (Experimental Procedures). Using this assay, the level of contamination of H_4-PteGlu$_5$ in the 10-CHO-H_4PteGlu$_5$ solution was less than 0.05%, suggesting that this cannot be the cause of the effect of SHMT and serine on the initial rate.

The other enzyme in the cytosol to use H_4PteGlu$_n$ as a substrate is the 10-CHO-THF synthetase activity of the trifunctional enzyme C_1-tetrahydrofolate synthase (Strong & Schirch, 1989). This enzyme catalyzes the formation of 10-CHO-H_4PteGlu$_n$ from MgATP, formate, and H_4PteGlu$_n$

(Scheme 1). When these substrates were flowed against 10-CHO-THF dehydrogenase, an initial velocity increased 3.0-fold was observed compared to the 10-CHO-THF dehydrogenase reaction alone (Figure 3, line 3). Again, the reaction remained linear for long periods of time. This increased initial velocity was dependent on C_1-THF synthase since addition of only the substrates MgATP and formate had no effect on the initial rate of the 10-CHO-THF dehydrogenase catalysis of reaction 1. When this reaction was repeated in a conventional spectrophotometer with 10-CHO-H_4PteGlu$_5$, the initial rate was increased 2.4-fold (Figure 4).

Even though the isolated 10-CHO-THF dehydrogenase does not contain bound H_4PteGlu$_5$, it may contain some other bound inhibitor which is removed by either SHMT or C_1-THF synthase, resulting in the increased initial rate effects. To test, this we took advantage of the fact that SHMT binds to CM-Sephadex at pH 6.8 but 10-CHO-THF dehydrogenase passes through the column under these conditions. We first incubated purified 10-CHO-THF dehydrogenase with SHMT and L-serine at pH 6.8 for 5 min which would remove any bound inhibitor present. The solution was then passed through a small 1 × 5 cm CM-Sephadex column to remove the SHMT. The resulting 10-CHO-THF dehydrogenase was then assayed for dehydrogenase activity with and without SHMT and serine in the assay buffer. We observed the same 1.8-fold increase in the initial rate in the presence of SHMT and serine that was observed with 10-CHO-THF dehydrogenase which had not been preincubated with this enzyme.

Addition of either SHMT and L-serine or MgATP, formate, and C_1-tetrahydrofolate synthase had no effect on the initial rate of the propanal dehydrogenase activity of 10-CHO-THF dehydrogenase (eq 3) (Figure 4). Previous investigators have shown that the substrate analog 10-CHO-5,8-dideazafolate is also a good substrate for both the dehydrogenase and hydrolase activities of 10-CHO-THF dehydrogenase (Krupenko et al., 1995). When this substrate analog was used and the effect of the addition of SHMT and serine tested, neither relief of product inhibition nor an increase in initial rate was observed. This is consistent with the product 5,8-dideazafolate not being a substrate for SHMT. A slight activation of about 1.2-fold was observed by the addition of C_1-tetrahydrofolate synthase when 10-CHO-5,8-dideazafolate was used as the substrate (Figure 4).

Folate Binding Properties of 10-CHO-THF Dehydrogenase. These experiments were designed to determine the tight binding stoichiometry of H_4PteGlu$_5$ to 10-CHO-THF dehydrogenase and to determine if 10-CHO-H_4PteGlu$_5$ is also bound tightly to 10-CHO-THF dehydrogenase. 10-CHO-THF dehydrogenase was incubated with 10-^{14}CHO-H_4PteGlu$_5$ in the presence and absence of $NADP^+$ in Tris buffer at pH 7.5. For the reaction not using $NADP^+$, 2-mercaptoethanol was replaced with 1 mM DTT and the reaction maintained at 4 °C. It was immediately placed on a Sephadex G-25 column at 4 °C and eluted with the equilibration Tris buffer in less than 15 min. The hydrolase activity is dependent on high concentrations of 2-mercaptoethanol which is used at 100 mM in assaying for this activity (Schirch et al., 1994). Under the conditions of no 2-mercaptoethanol and $NADP^+$ and low temperature, the hydrolase activity should be very low and only a small percent of the 10-CHO-H_5PteGlu$_5$ would be converted to H_4PteGlu$_5$ during the experiment. If the substrate 10-CHO-H_4PteGlu$_5$ binds tightly to the enzyme, it should elute with the protein. The eluate was collected and analyzed for absorbance at 280 nm and radioactivity of the formyl group. Figure 5A shows that the protein (solid circles) eluted without any radioactivity (open squares).

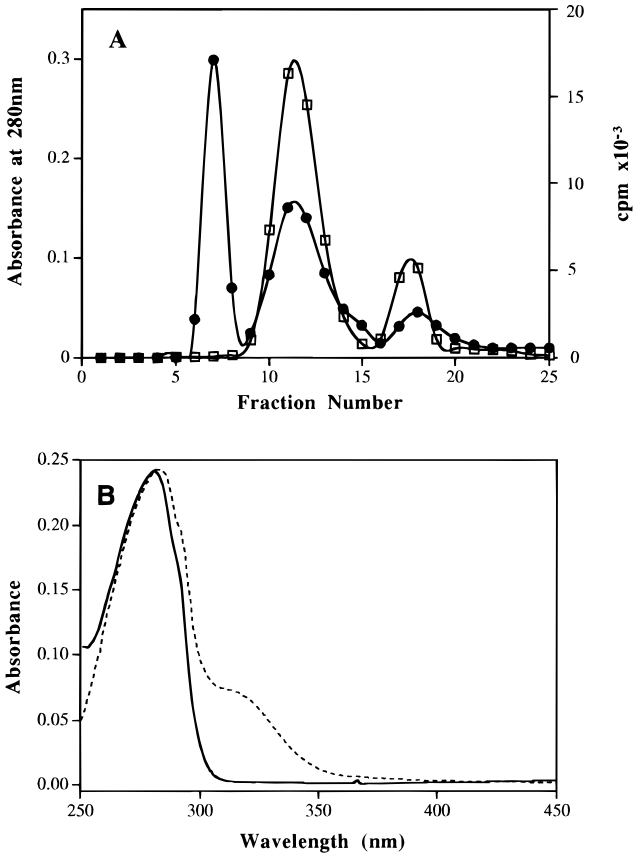

FIGURE 5: Tight binding of H_4PteGlu$_5$ to 10-CHO-THF dehydrogenase. (A) 10-^{14}CHO-H_4PteGlu$_5$ (13 nmol) was added to 2.5 nmol of 10-CHO-THF dehydrogenase in 50 mM Tris/HCl at pH 7.7 and 4 °C containing 1 mM DTT. The solution was immediately chromatographed on a 1 × 20 cm column of BioGel P-6DG in the same buffer at 4 °C. Aliquots (0.6 mL) were collected and analyzed for radioactivity (open squares) and absorbance at 280 nm (filled circles). (B) Spectrum of combined fractions 6−8 (dashed line). Spectrum of purified 10-CHO-THF dehydrogenase without preincubation with any folates (solid line). The two spectra do not represent the same amount of protein. There is less protein in the complex (dashed line) than in the enzyme alone (solid line) since some of the absorbance at 280 nm is attributable to the bound H_4-PteGlu$_5$.

Figure 5A shows three resolved 280 nm absorbing elution peaks. Only the fractions from the last two of these contained radioactivity. The spectra of the fractions for each of the three peaks were analyzed. Figure 5B (dashed line) shows that the first eluting peak is protein with a shoulder at 310 nm, indicating the presence of bound H_4PteGlu$_5$. This is in contrast to the purified 10-CHO-THF dehydrogenase used in this experiment which shows no absorption above 300 nm (solid line in Figure 5B). The folate bound to the enzyme is not the substrate 10-CHO-H_4PteGlu$_5$ since no radioactivity was present. It was confirmed to be H_4PteGlu$_5$ by its ability to form a ternary complex with SHMT and glycine that absorbs at 495 nm [Schirch (1975) and Figure 7 of this study].

The second eluting peak exhibited the spectrum of 10-CHO-H_4PteGlu$_5$ (absorption maximum at 288 nm) rather than that of the product H_4PteGlu$_5$ (absorption maximum at 298 nm). This shows that most of the 10-CHO-H_4PteGlu$_5$

Table 2: Stoichiometry of Tight-Binding $H_4PteGlu_5$ and 5,8-Dideazatetrahydrofolate Polyglutamates to 10-Formyltetrahydrofolate Dehydrogenase

ligand complexed to 10-CHO-THF dehydrogenase	added ligand[a]	nanomoles of product bound/nanomoles of 10-CHO-THF dehydrogenase subunit	
		[^{14}C]glutamate[b]	A_{316nm}[c]
$H_4PteGlu_5$	none	−	1.15 ± 0.05
DDF-[^{14}C]Glu_4[d]	none	0.55	0.65
DDF-[^{14}C]Glu_4	DDF-Glu_4	0.008	0.84
DDF-[^{14}C]Glu_4	10-CHO-DDF-Glu_4	0.25	0.45

[a] The 10-CHO-THF dehydrogenase complex was incubated for 5 min with the added ligand before passing through a Sephadex G-25 column. [b] The stoichiometry of binding was determined from the specific radioactivity of the bound coenzyme. [c] The stoichiometry of binding was determined from the absorbance at 316 nm as described in Experimental Procedures. [d] DDF-Glu_4 is the tetraglutamate derivative of 5,8-dideazafolate.

had not been converted to product during the experiment. The third eluting peak did not exhibit an absorption maximum above 250 nm. The small amount of radioactivity may reflect [^{14}C]formate formed from several turnovers of the reaction.

When 10-CHO-THF dehydrogenase was preincubated with 10-CHO-$H_4PteGlu_5$ and $NADP^+$ for 10 min prior to passing through the molecular sieve column, the same results as recorded in Figure 5 were obtained except the second absorbing peak now exhibited the spectrum of the product $H_4PteGlu_5$ rather than that of 10-CHO-$H_4PteGlu_5$ (data not shown).

From a difference spectrum of a 5-fold excess of 10-CHO-THF dehydrogenase to $H_4PteGlu_5$, the spectral properties of the bound $H_4PteGlu_5$ were shown to be very similar to those of the unbound substrate (data not shown). There was a small shift in absorbance maximum of the bound form from 298 to 300 nm. Using the extinction coefficient at 280 and 316 nm of the bound $H_4PteGlu_5$, the concentrations of 10-CHO-THF dehydrogenase and the bound $H_4PteGlu_5$ were determined from the spectrum shown in Figure 5B (see Experimental Procedures). The results of multiple analyses showed that each subunit binds one $H_4PteGlu_5$ molecule (Table 2).

10-CHO-THF dehydrogenase with the tightly bound $H_4PteGlu_5$ was tested for activity using the assays for reactions 1−3 (eqs 1−3). The enzyme showed complete activity when $NADP^+$ and propanal were used as substrates (eq 3). Unexpectedly, the enzyme also showed normal activity when 10-CHO-$H_4PteGlu_5$ was used as substrate in either reaction 1 or 2. This suggests that, even though the product of these two reactions is tightly bound to the enzyme, it does not interfere with 10-CHO-THF dehydrogenase activity. This raises the question of whether the tight-binding folate site is separate from the catalytic site.

5,8-Dideazafolate Bound to 10-CHO-THF Dehydrogenase. 10-CHO-THF dehydrogenase was incubated with [^{3}H]-glutamate-labeled 5,8-dideazafolate tetraglutamate. After size exclusion chromatography, there was a common elution of radioactivity and protein (data not shown). The spectrum and radioactivity of the protein showed that about 0.6 equiv of 5,8-dideazafolate was bound per subunit of enzyme (Table 2). This enzyme was then divided into three equal aliquots. The first aliquot was chromatographed a second time on the size exclusion column. More than 80% of the radioactivity remained bound to 10-CHO-THF dehydrogenase, showing that it was tightly bound. The second aliquot was incubated with a 20-fold excess of unlabeled 5,8-dideazafolate tetraglutamate for 5 min and then passed down the size exclusion column. The protein peak contained less than 2% of the radioactivity of the original sample, but the spectrum showed that it contained slightly more bound 5,8-dideazafolate (Table 2). The third aliquot was incubated for 5 min with a 20-fold excess of unlabeled 10-CHO-5,8-dideazafolate tetraglutamate before chromatography. The eluted protein contained about 50% of the radiolabel of the original sample but about 0.7 equiv of the amount of bound 5,8-dideazafolate tetraglutamate. These results suggest that the polyglutamate form of 5,8-dideazafolate binds tightly to 10-CHO-THF dehydrogenase. The results also show that, even though the 5,8-dideazafolate tetraglutamate is bound tightly, it is in equilibrium with added product. What is somewhat surprising is that the tightly bound product is more slowly displaced by the substrate 10-CHO-5,8-dideazafolate tetraglutamate.

10-CHO-THF Dehydrogenase·$H_4PteGlu_5$ Complex as a Source of $H_4PteGlu_5$ for SHMT and C_1-THF Synthase. The results in Figures 3 and 4 show the effect of SHMT and C_1-THF synthase on the activity of 10-CHO-THF dehydrogenase in the presence of excess 10-CHO-$H_4PteGlu_5$. However, in the cell, it appears that the enzymes exist at higher concentrations than their folate substrates. We have previously shown that SHMT and the three reactions catalyzed by C_1-THF synthase form a metabolic cycle in which the folate substrates serve in catalytic concentrations (Strong & Schirch, 1989; Kruschwitz et al., 1994). These reactions are shown as cycle 1 in Scheme 1. When an excess of SHMT and C_1-THF synthase (5−10-fold) are used with respect to the concentration of any one of the folate intermediates, the rate of cycle 1, as determined by NADPH oxidation, in the conversion of formate to serine is directly proportional to the concentration of the folate substrate (Strong & Schirch, 1989; Kruschwitz et al., 1994). We have repeated this study, and under the conditions used, the free added $H_4PteGlu_5$ substrate is being cycled about 50 times per minute (Figure 6, closed circles).

The 10-CHO-THF dehydrogenase·$H_4PteGlu_5$ complex, as eluted from the size exclusion column shown in Figure 5B, was used as a source of the substrate for cycle 1 in place of free $H_5PteGlu_5$. If the two enzymes acted independently of each other, you would expect one of two possible results to this experiment. First, the tightly bound $H_4PteGlu_5$ would not dissociate from the 10-CHO-THF dehydrogenase complex and no observed NADPH oxidation would be observed. Second, since the K_d for the 10-CHO-THF dehydrogenase·$H_4PteGlu_5$ complex (about 15 nM) is 1 order of magnitude lower than the K_d for either the SHMT·$H_4PteGlu_5$ or C_1-THF synthase·$H_4PteGlu_5$ complex (100−200 nM; Strong & Schirch, 1989), the $H_4PteGlu_5$ would be released slowly and only partially from 10-CHO-THF dehydrogenase, resulting in a lag in the appearance of NADPH and a greatly decreased rate of the cycle. We observed that the rate of NADPH production exhibited no lag and the rate of cycle 1 (Scheme 1) proceeded as though all of the $H_4PteGlu_5$ of the 10-CHO-THF dehydrogenase·$H_4PteGlu_5$ complex had been transferred to SHMT and C_1-THF synthase (Figure 6, open squares). This suggests that all of the $H_4PteGlu_5$ in the 10-CHO-THF

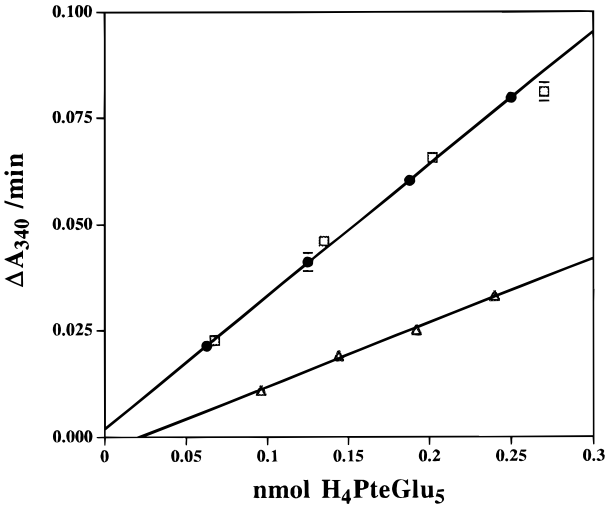

FIGURE 6: Relationship of the rates of cycles 1 and 2 (Scheme 1) with increasing concentrations of $H_4PteGlu_5$. (●) $H_4PteGlu_5$ was added as 5,10-CH^+-$H_4PteGlu_5$ to a solution containing 2.7 nmol of cytosolic SHMT and 1.3 nmol of C_1-THF synthase and required cosubstrates: 200 μM NADPH, 2 mM MgATP, 4 mM formate, and 20 mM glycine (cycle 1). (□) The addition of $H_4PteGlu_5$ was as the 10-CHO-THF dehydrogenase complex isolated from a size exclusion column as shown by the spectrum in Figure 5B. (△) The addition of the 10-CHO-$H_4PteGlu_5$ to a solution containing 1.3 nmol of C_1-THF synthase and 1.5 nmol of 10-CHO-THF dehydrogenase with appropriate cosubstrates $NADP^+$, formate, and MgATP (cycle *2*, Figure 5).

dehydrogenase·$H_4PteGlu_5$ complex was released to SHMT and C_1-tetrahydrofolate synthase.

The combination of 10-CHO-THF dehydrogenase and C_1-THF synthase also catalyzes a cycle in which 10-CHO-$H_4PteGlu_5$ and $H_4PteGlu_5$ function at catalytic levels (cycle 2, Scheme 1). Each cycle reduces 1 equiv of $NADP^+$ to NADPH. The cycle catalyzes the ATP-dependent oxidation of formate to CO_2. To determine if the tightly bound $H_4PteGlu_5$ in the 10-CHO-THF dehydrogenase·$H_4PteGlu_5$ complex could serve as the coenzyme in cycle 2, the complex was added to an equal amount of C_1-THF synthase and excess ATP, formate, and $NADP^+$. The rate of cycle 2 was linear with increasing concentrations of the 10-CHO-THF dehydrogenase·$H_4PteGlu_5$ complex (Figure 6, open triangles). The cycle was operating at 25 cycles min^{-1}. With excess 10-CHO-$H_4PteGlu_5$, the k_{cat} for reaction 1 is 52 min^{-1}. This lower value for k_{cat} in the cycle compared to that for the 10-CHO-THF dehydrogenase reaction alone may be due to the C_1-THF synthase being the rate-controlling step in the cycle.

Rate of Transfer of 10-CHO-THF Dehydrogenase-Bound $H_4PteGlu_5$ to SHMT. The results presented in Figure 6 suggest that the tightly bound $H_4PteGlu_5$ is transferred from 10-CHO-THF dehydrogenase to both SHMT and C_1-THF synthase in less than the 5 s required for mixing. The rate of this transfer of $H_4PteGlu_5$ can be determined with SHMT by taking advantage of a unique property of this enzyme. The SHMT·Gly·$H_4PteGlu_5$ ternary complex exhibits a sharp absorption peak at 496 nm with an extinction coefficient of nearly 40 mM^{-1} cm^{-1} (Schirch, 1975). The rate of formation of this ternary complex from $H_4PteGlu$, glycine, and SHMT is greater than 200 s^{-1} (Schirch, 1975). Scheme 2 illustrates how trapping the released $H_4PteGlu_5$ by excess SHMT·Gly would shift the equilibrium toward the formation of the SHMT·$H_4PteGlu_5$·Gly. We have followed the formation of

Scheme 2: Model for Determining the Rate of Transfer of $H_4PteGlu_5$ from the 10-CHO-THF Dehydrogenase·$H_4PteGlu_5$ Complex to SHMT·Gly in the Presence and Absence of 5,8-Dideazafolate[a]

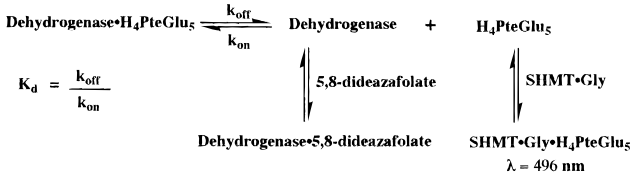

[a] k_{on} and k_{off} are the rate of formation and dissociation of $H_4PteGlu_5$ from the complex, respectively. The value for k_{on} can be estimated from the values for K_d and k_{off}.

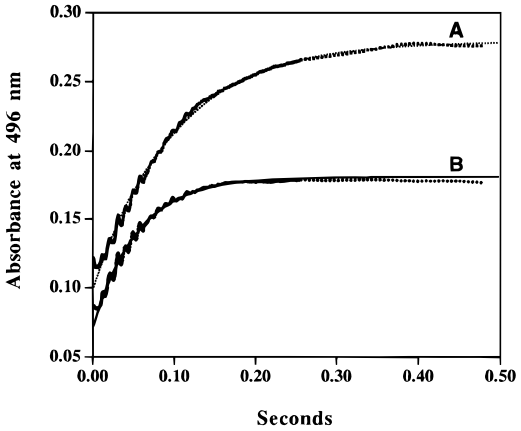

FIGURE 7: Rate of transfer of $H_4PteGlu_5$ from the 10-CHO-THF dehydrogenase·$H_4PteGlu_5$ complex to SHMT. To one syringe of a stopped-flow spectrophotometer was added 10 μM FTD·$H_4PteGlu_5$ in 50 mM potassium phosphate at pH 7.3. (Curve A) To the second syringe were added 80 μM SHMT, 30 mM glycine, and 100 μM 5,8-dideazafolate in the same buffer. The absorbance of the reacting solutions was monitored at 496 nm which is the absorption maximum of the SHMT·Gly·$H_4PteGlu_5$ ternary complex. (Curve B) Same conditions as curve A except no 5,8-dideazafolate was included. The 5,8-dideazafolate does not form a complex with SHMT that absorbs at 496 nm.

this ternary complex in a stopped-flow spectrophotometer by flowing the 10-CHO-THF dehydrogenase·$H_4PteGlu_5$ complex (10 μM) in one syringe against a solution of SHMT (80 μM) saturated with glycine (30 mM) in the second syringe (Figure 7). There is a rapid first-order increase in the formation of the ternary SHMT·Gly·$H_4PteGlu_5$ complex with a rate constant of 25 s^{-1} at 23 °C (Figure 7, curve B). This rate constant did not change appreciably with SHMT concentration, although we could not decrease the concentration below 10 μM SHMT because the amplitude became too small. The rate of formation of the SHMT·Gly·$H_4PteGlu_5$ complex of 25 s^{-1} at 23 °C must be the rate of dissociation of $H_4PteGlu_5$ from the 10-CHO-THF dehydrogenase·$H_4PteGlu_5$ complex (k_{off} in Scheme 2). This rate is much larger than the k_{cat} of 0.9 s^{-1} for 10-CHO-THF dehydrogenase at 30 °C.

Under the conditions of the experiment, 80 μM SHMT and 10 μM 10-CHO-THF dehydrogenase·$H_4PteGlu_5$ complex, 50% of the $H_4PteGlu_5$ was transferred to SHMT as determined from the ϵ_{496} for the ternary complex. That 50% of the $H_4PteGlu_5$ remained to the dehydrogenase was verified by adding 100 μM 5,8-dideazafolate to the syringe with SHMT. This product analog would be expected to bind to 10-CHO-THF dehydrogenase and displace all the $H_4PteGlu_5$ as shown in Scheme 2. However, 5,8-dideazafolate does not form a complex with SHMT and glycine and does not

result in an increase in absorbance at 496 nm. In this experiment, the amplitude of the absorbance at 496 nm was almost double that observed without the addition of 5,8-dideazafolate, confirming that the remaining $H_4PteGlu_5$ had been released from 10-CHO-THF dehydrogenase (Figure 7, curve A). Of considerable interest was the result when 10-CHO-5,8-dideazafolate replaced 5,8-dideazafolate in this experiment. There was not a rapid additional increase in amplitude at 496 nm, and the results looked very much like curve B shown in Figure 7. However, there was a slow increase in amplitude after the initial rapid phase, taking about 15 min to reach completion and resulting in the release of more than 90% of the bound $H_4PteGlu_5$ from the 10-CHO-THF dehydrogenase·$H_4PteGlu_5$ complex. This last experiment shows that 5,8-dideazafolate rapidly displaces the tightly bound $H_4PteGlu_5$ from the 10-CHO-THF dehydrogenase·$H_4PteGlu_5$ complex but that 10-CHO-5,8-dideazafolate displaces it very slowly. Most likely, the slow release of the tightly bound $H_4PteGlu_5$ occurs only when the 10-CHO-5,8-dideazafolate is slowly hydrolyzed to 5,8-dideazafolate.

DISCUSSION

The purification of 10-CHO-THF dehydrogenase in this study confirms that this enzyme exists in very high concentration in rabbit liver. Two rabbit livers (120 g), contain about 360 mg of 10-CHO-THF dehydrogenase, representing about 1.2% of the soluble protein (Table 1). Assuming that there is 0.7 mL of cell volume per gram of tissue, this would put the concentration of 10-CHO-THF dehydrogenase subunits in rabbit liver at about 42 μM. Previous studies have shown that the concentrations of SHMT and C_1-THF synthase subunits in rabbit liver total about 26 μM, giving a combined total concentration of folate binding sites of 68 μM for the three enzymes used in this study (Strong & Schirch, 1989). The total concentration of folylpolyglutamates in mammalian liver has been determined to be in the range of 25−35 μM (Cichowicz & Shane, 1987; Horne et al., 1989). There are other folate binding enzymes at high concentrations in mammalian cells. One example is glycine *N*-methyltransferase which binds 5-methyl-$H_4PteGlu_5$ tightly and is estimated to be about 1−3% of the soluble cytosolic proteins (Yeo & Wagner, 1992). It appears that the concentration of proteins in liver which have folylpolyglutamate binding sites may exceed the total concentration of folylpolyglutamates by as much as 5−10-fold. Since the K_d for folylpolyglutamates for many of these enzymes is in the 100 nM range, it seems that *in vivo* most of the folylpolyglutamate pool may be enzyme-bound.

Kinetic Properties of 10-CHO-THF Dehydrogenase. The determination of the K_m of the polyglutamate forms of 10-CHO-$H_4PteGlu_n$ for 10-CHO-THF dehydrogenase has not been published. This is primarily the result of the rapid decrease in activity observed with the polyglutamate forms of the substrate during the assay. Determination of a true initial velocity is very difficult in the low micromolar substrate concentration range. The decrease in the rate of an assay with time was believed to be due to product inhibition by $H_4PteGlu_n$. We provide evidence in this study that product inhibition does occur. First, we have determined the K_d for $H_4PteGlu_5$ from fluorescence titration experiments to be about 21 nM. Next, we analyzed the progress curve of both the hydrolase and dehydrogenase activity of 10-CHO-THF dehydrogenase with 10-CHO-$H_4PteGlu_5$. The rate of product formation could be fit by the equation for competitive product inhibition. The value of 15 nM obtained for the K_p of $H_4PteGlu_5$ is very close to the K_d of 21 nM obtained from the fluorescence titration experiment (Figures 1 and 2). Of most interest is the K_s of 0.9 μM for 10-CHO-$H_4PteGlu_5$ obtained from the product inhibition analysis. This K_s value is high compared to those of the other enzymes in the cell that use folylpolyglutamates as substrates.

Tight Binding. If only the kinetic properties of 10-CHO-THF dehydrogenase were investigated, it would appear as a normal enzyme except for binding its product much more tightly than its substrate. However, the observation that this enzyme binds its product $H_4PteGlu_5$ so tightly that it does not dissociate during size exclusion chromatography is difficult to reconcile with the kinetic studies. We addressed two questions about the tight binding of $H_4PteGlu_5$. First, what is the stoichiometry of tight binding, and second, what is the structural specificity for tight binding?

Under conditions where 10-CHO-$H_4PteGlu_5$ would be hydrolyzed very slowly, it was observed that only the product $H_4PteGlu_5$ remained bound to the enzyme after size exclusion chromatography (Figure 5). There was enough time during chromatography for several catalytic turnovers of the hydrolase activity, but the substrate would have been in large excess at all times compared to the amount of product. We conclude that for the pure enzyme the product is much preferred at the tight binding site. This is different than what was observed by Wagner et al. (1995), who found that in a liver homogenate the substrate appears to be bound tightly and is only slowly converted in hours to the product. We have also shown that the product analog 5,8-dideazafolate binds tightly to the enzyme. Again, there is no evidence that the substrate analog 10-CHO-5,8-dideazafolate binds tightly to 10-CHO-THF dehydrogenase.

Kinetic Properties of Tight Binding. Tight binding by definition means that the rate of dissociation is very slow. One would expect that a tightly bound product would block the binding of substrate and thus inhibit the enzyme. This is not the case with 10-CHO-THF dehydrogenase. We could detect no differences in steady-state kinetic properties between enzyme with or without bound $H_4PteGlu_5$. This produces the question of whether the $H_4PteGlu_5$ tight binding site is separate from the catalytic site. We have no method to determine if in the first turnover of the catalytic site the $H_4PteGlu_5$ is released free in solution or if it binds tightly to another site.

The possibility that binding of the substrate results in rapid release of product from the 10-CHO-THF dehydrogenase·$H_4PteGlu_5$ complex does not appear to be the explanation for the normal steady-state kinetic pattern. First, when the 10-CHO-THF dehydrogenase·$H_4PteGlu_5$ complex was reacted with SHMT·glycine, about 50% of the $H_4PteGlu_5$ was rapidly released from the 10-CHO-THF dehydrogenase complex (Figure 7, curve B). However, the addition of 10-CHO-5,8-dideazafolate did not result in the rapid release of the remaining 50% of tightly bound $H_4PteGlu_5$. A second experiment supports this observation. The addition of unlabeled 10-CHO-5,8-dideazafolate tetraglutamate to the glutamate-labeled 10-CHO-THF dehydrogenase·5,8-dideazafolate tetraglutamate complex did not result in rapid loss of the bound labeled 5,8-dideazafolate (Table 2).

Even though the substrate does not cause the rapid release of bound product, the addition of excess product does result in rapid release. The first evidence for this was the exchange of the ^{14}C-labeled 5,8-dideazafolate tetraglutamate with unlabeled 5,8-dideazafolate tetraglutamate (Table 2). The effect of excess product on the rate of product dissociation was further confirmed by the ability of 5,8-dideazafolate to release the last 50% of the tightly bound $H_4PteGlu_5$ in the presence of SHMT and glycine (Figure 7, curve A). This rapid equilibrium between bound and unbound $H_4PteGlu_5$ would also explain why a linear Scatchard plot could be obtained as shown in Figure 1. The linearity of this plot can result only if there is an equilibrium between bound and unbound forms of the coenzyme.

Both SHMT and C_1-THF synthase can cause the rapid release of the tightly bound $H_4PteGlu_5$. Stopped-flow analysis of the transfer of $H_4PteGlu_5$ from the 10-CHO-THF dehydrogenase·$H_4PteGlu_5$ complex to form the SHMT·Gly·$H_4PteGlu_5$ complex clearly shows the effect of SHMT (Figure 7). The rate of this transfer exceeds by at least 25-fold the k_{cat} of the 10-CHO-THF dehydrogenase catalysis of reaction 1 (eq 1). If the K_p for $H_4PteGlu_5$ is 20 nM, as determined from the product inhibition analysis and the fluorescence titration experiment, the k_{on} for binding of $H_4PteGlu_5$ would be 1×10^9 M^{-1} s^{-1} (Scheme 2). This on rate for forming the 10-CHO-THF dehydrogenase·$H_4PteGlu_5$ complex exceeds the accepted value for the diffusion-controlled rate by about 1 order of magnitude, suggesting that the K_p for $H_4PteGlu_5$ is higher than 20 nM in the presence of SHMT. To have a value for k_{on} of 1×10^8 M^{-1} s^{-1} would require a K_p for $H_4PteGlu_5$ of 250 nM. These results suggest that the model presented in Scheme 2 cannot explain the mechanism of transfer of $H_4PteGlu_5$ between 10-CHO-THF dehydrogenase and SHMT.

The ability of SHMT to increase the rate of release of product may also explain its effect on the initial velocity of the dehydrogenase and hydrolase activities of 10-CHO-THF dehydrogenase (Figures 3 and 4). If k_{cat} is partially determined by the rate of product release, then SHMT increasing the rate of release would result in an increase in k_{cat}. A similar argument can be made for the effect of C_1-THF synthase.

The effect of SHMT and C_1-THF synthase on initial velocity and the increased rate of dissociation of the 10-CHO-THF dehydrogenase·$H_4PteGlu_5$ complex also help to explain the results recorded in Figure 6. Under conditions where SHMT and C_1-THF synthase are in excess of the 10-CHO-THF dehydrogenase·$H_4PteGlu_5$ complex, it appears that all of the $H_4PteGlu_5$ is released to function in cycle 1 (Scheme 1). The apparent complete transfer of the $H_4PteGlu_5$ to SHMT and C_1-THF synthase from the 10-CHO-THF dehydrogenase·$H_4PteGlu$ complex suggests that these enzymes not only increase the rate of release of product but also change the affinity of 10-CHO-THF dehydrogenase for its product. Even if the value of 20 nM for the K_d of the 10-CHO-THF dehydrogenase·$H_5PteGlu_5$ complex (Figures 1 and 2) is correct, this is still 2 orders of magnitude lower than the K_d of 100−200 nM of either SHMT or C_1-THF synthase for $H_4PteGlu_5$ (Strong & Schirch, 1989). However, as noted above, the k_{off} of 25 s^{-1} obtained for the rate of transfer of $H_4PteGlu_5$ from 10-CHO-THF dehydrogenase to SHMT requires a K_p of greater than 250 nM if k_{on} is to be near the limit of the diffusion-controlled value for k_{on} of 1×10^8 M^{-1} s^{-1}. This further suggests that the K_d for the 10-CHO-THF dehydrogenase·$H_4PteGlu_5$ complex must be larger than 20 nM in the presence of SHMT.

In conclusion, the individual properties of purified 10-CHO-THF dehydrogenase, C_1-THF synthase, and SHMT suggest that in competition for $H_4PteGlu_5$ the 10-CHO-THF dehydrogenase would dominate because its affinity for $H_4PteGlu_5$ is 1 order of magnitude higher, as determined from the product inhibition studies. Also, its ability to bind $H_4PteGlu_5$ tightly, which requires a very slow dissociation rate, would further suggest that 10-CHO-THF dehydrogenase would compete with SHMT and C_1-THF synthase for free $H_4PteGlu_5$. However, when combined, the three enzymes appear to behave as though SHMT and C_1-THF synthase have the higher affinity and that the rate of release of $H_4PteGlu_5$ from the 10-CHO-THF dehydrogenase complex is rapid. At this time, we have no model or mechanism to explain these results. It would seem that the explanation will require some physical interaction between 10-CHO-THF dehydrogenase, SHMT, and C_1-THF synthase. Also, unresolved are the mechanism of the apparent exchange of tightly bound $H_4PteGlu_5$ with free $H_4PteGlu_5$ and the lack of inhibition of catalytic activity when the product is tightly bound. These mechanistic questions are the focus of our current studies. We must first determine if there are separate catalytic and folate tight binding sites on 10-CHO-THF dehydrogenase.

Physiological Function of 10-CHO-THF Dehydrogenase. The physiological function of 10-CHO-THF dehydrogenase is not clear. Krebs et al. (1976) originally suggested that it served a regulation function by disposing of excess one-carbon units from 10-CHO-$H_4PteGlu_5$ to regenerate $H_4PteGlu_5$. This is supported by the recent observations of Champion et al. (1994), who have analyzed the folate pools in a mouse strain which lacks 10-CHO-THF dehydrogenase. The homozygous mutant mice have a 35% reduction in their liver cell total folate pool with a 2.5-fold increase in the level of 10-CHO-$H_4PteGlu_n$ and a 4-fold reduction in the level of $H_4PteGlu_n$. These three observations support the notion that 10-CHO-THF dehydrogenase serves as an important site of binding of folylpolyglutamates in liver and regulates the interconversion of 10-CHO-$H_4PteGlu_n$ and $H_4PteGlu_n$. The product inhibition pattern observed in Figure 2 would support a role for 10-CHO-THF dehydrogenase in regulating the interconversion of 10-CHO-$H_4PteGlu_n$ and $H_4PteGlu_n$. Product inhibition has been characterized in a number of ATP-utilizing enzymes (Atkinson, 1970). Atkinson has discussed how these enzymes respond to the "energy charge" in the cell which relates to the ratio of ATP, ADP, and AMP concentrations. In the same sense, 10-CHO-$H_4PteGlu_n$ represents a high-energy form of formyl groups which are required for several biosynthetic enzymes. One role of 10-CHO-THF dehydrogenase may be to regulate the "high-energy formyl charge" of the cell. This would be in agreement with the studies of Appling which show the importance of formate in one-carbon metabolism (Pasternack et al., 1994; Barlowe & Appling, 1989). Recently, a 10-formyltetrahydrofolate hydrolase has been purified and characterized from *Escherichia coli* (Nagy et al., 1995). This enzyme shows heterotropic cooperativity by glycine and methionine showing a direct connection to regulation of the

folate pool by one-carbon metabolites. In liver, the regulation mechanism may be product inhibition rather than heterotropic cooperativity.

Neymeyer and Tephly (1994) have suggested that 10-CHO-THF dehydrogenase plays an important role in removing formate formed during methanol toxicity. Methanol is oxidized to formate which is toxic to the cell. Rats are not as susceptible to methanol poisoning as humans, presumably because the excess formate formed from methanol can be removed by oxidation to CO_2 by 10-CHO-THF dehydrogenase. These authors showed that target tissues of methanol poisoning, such as retina, optic nerve, and brain, contain 10-CHO-THF dehydrogenase in the rat. However, Smith and Taylor (1982) have shown that in mice there is not a correlation between folate deficiency and methanol toxicity. Rather, excretion of formate may be the key factor in differences of methanol toxicity.

REFERENCES

Atkinson, D. E. (1970) in *The Enzymes* (Boyer, P., Ed.) 3rd ed., 1970, Vol. 1, pp 461−491, Academic Press, New York.

Barlowe, C. K., & Appling, D. R. (1988) *BioFactors 1*, 171−176.

Champion, K. M., Cook, R. J., Tollaksen, S. L., & Giometti, C. S. (1994) *Proc. Natl. Acad. Sci. U.S.A. 91*, 11338−11342.

Chen, M. S., & Schirch, L. (1973) *J. Biol. Chem. 248*, 3631−3635.

Cichowicz, D. J., & Shane, B. (1987) *Biochemistry 26*, 504−512.

Cook, R. J., & Wagner, C. (1982) *Biochemistry 21*, 4427−4434.

Cook, R. J., & Wagner, C. (1986) *Methods Enzymol. 122*, 251−255.

Cook, R. J., Lloyd, R. S., & Wagner, C. (1991) *J. Biol. Chem. 266*, 4965−4973.

Grimshaw, C. E., Henderson, G. B., Soppe, G. G., Hansen, G., Mathur, E. J., & Huennekens, F. M. (1984) *J. Biol. Chem. 259*, 2728−2733.

Horne, D. W., Patterson, D., & Cook, R. J. (1989) *Arch. Biochem. Biophys. 270*, 729−733.

Krebs, H. A., Hems, R., & Tyler, B. (1976) *Biochem. J. 158*, 341−353.

Krupenko, S. A., Wagner, C., & Cook, R. J. (1995) *Biochem. J. 306*, 651−655.

Kruschwitz, H. L., McDonals, D., Cossins, E. A., & Schirch, V. (1994) *J. Biol. Chem. 269*, 28757−28763.

Kutzbach, C., & Stokstad, E. L. R. (1971) *Methods Enzymol. 18B*, 793−798.

Min, H., Shane, B., & Stokstad, E. L. R. (1988) *Biochim. Biophys. Acta 967*, 348−353.

Moran, R. G., & Colman, P. D. (1984) *Biochemsitry 23*, 4580−4589.

Nagy, P. L., Marolewski, A., Benkovic, S. J., & Zalkin, H. (1995) *J. Bacteriol. 177*, 1292−1298.

Neymeyer, V. R., & Tephly, T. R. (1994) *Life Sci. 54*, 395−399.

Pasternack, L. B., Laude, D. A., & Appling, D. R. (1994) *Biochemistry 33*, 74−82.

Rios-Orlandi, E. M., Zarkadas, C. G., & MacKenzie, R. E. (1986) *Biochim. Biophys. Acta 871*, 24−35.

Schirch, D., Villar, E., Maras, B., Barra, D., & Schirch, V. (1994) *J. Biol. Chem. 269*, 24728−24735.

Schirch, L. (1975) *J. Biol. Chem. 250*, 1939−1945.

Schirch, L. (1982) *Adv. Enzymol. Relat. Areas Mol. Biol. 53*, 83−112.

Scrutton, M. C., & Beis, I. (1979) *Biochem. J. 177*, 833−846.

Segel, I. H. (1975) in *Enzyme Kinetics*, pp 120−125, John Wiley & Sons, New York.

Smith, E. N., & Taylor, R. T. (1982) *Toxicology 25*, 271−287.

Stover, P., & Schirch, V. (1992) *Anal. Biochem. 202*, 82−88.

Strong, W. B., & Schirch, V. (1989) *Biochemistry 28*, 9430−9439.

Wagner, C., Briggs, W. T., Horne, D. W., & Cook, R. J. (1995) *Arch. Biochem. Biophys. 316*, 141−147.

Webb, J. L. (1963) *Enzyme and Metabolic Inhibitors*, Vol. I, pp 71−75, Academic Press, New York.

Yeo, E. J., & Wagner, C. (1992) *J. Biol. Chem. 267*, 24669−24674.

BI9619684